Werk

Jahr: 1981
Kollektion: fid.geo
Signatur: 8 Z NAT 2148:49
Digitalisiert: Niedersächsische Staats- und Universitätsbibliothek Göttingen
Werk Id: PPN1015067948_0049
PURL: http://resolver.sub.uni-goettingen.de/purl?PPN1015067948_0049

LOG Id: LOG_0033
LOG Titel: Propagation of surface waves in marine sediments
LOG Typ: article

Übergeordnetes Werk

Werk Id: PPN1015067948
PURL: http://resolver.sub.uni-goettingen.de/purl?PPN1015067948
OPAC: http://opac.sub.uni-goettingen.de/DB=1/PPN?PPN=1015067948

Contact

Niedersächsische Staats- und Universitätsbibliothek Göttingen
Georg-August-Universität Göttingen
Platz der Göttinger Sieben 1
37073 Göttingen
Germany
Email: gdz@sub.uni-goettingen.de

J Geophys (1981) 49:115–122

Journal of Geophysics

Propagation of Surface Waves in Marine Sediments

H.-H. Essen, H. Janle, F. Schirmer, and J. Siebert
Institut für Geophysik, Universität Hamburg, Bundesstr. 55, D-2000 Hamburg 13, Federal Republic of Germany

Abstract. In 1977 seismic investigations were carried out on the shore belt of the North Sea in order to observe slow surface waves. The water depth was about 1 m. Most of the seismic sections show two wave groups with a mean frequency of 4 Hz and velocities of 100 and 230 ms^{-1}. The axial ratios of horizontal to vertical amplitude are 0.5 and 2.3, respectively. Some seismograms are analysed by multiple filter techniques. By means of least-squares fits the observed and theoretical group-velocity curves are compared. It turns out that a simple two-layer model of the sedimentary sea floor yields reasonable results with respect to group velocities but not with respect to the axial ratios of horizontal and vertical amplitudes. This discrepancy is overcome by introducing an additional near-surface layer of lower shear-wave velocity. The final model consists of a water layer (1 m) and three sedimentary layers (3 m, 15 m, ∞) with shear-wave velocities of 75 ms^{-1}, 150 ms^{-1}, and 250 ms^{-1}, respectively.

Key words: Shear-wave velocities – Marine sediments – Interface waves – Multiple-filter technique – Model computations

Introduction

Interest in sedimentary shear-wave velocities has increased considerably during recent years (Essen 1977; Hawker 1979) particularly with reference to underwater acoustics. Low-velocity shear waves may be responsible for energy losses in the acoustic waveguide, and the amount of loss depends strongly on the shear-wave velocity. Shear-wave velocities in marine sediments are also of importance in other geophysical problems but there is still a great lack of measured data. This is due mainly to experimental difficulties. A detailed discussion of this subject is given by Hamilton (1976) and will not be repeated here.

In seismology Rayleigh waves, which propagate along the free surface, are of great importance for determining the elastic parameters of the upper mantle. Similar methods may be applied for the measurement of shear-wave velocities in the upper layers of ocean sediments. Following Cagniard (1962) we call the surface waves existing at the boundary between a fluid and a solid Scholte waves, so as to distinguish from Stoneley waves which propagate along a solid-solid interface.

In the case of homogeneous halfspaces both Rayleigh and Scholte waves are nondispersive. In the presence of layers, however, the Rayleigh as well as the Scholte wave splits up into a finite number of dispersive modes. This effect is important for the interpretation of the experimental results presented in this paper.

Surface-wave measurements at the sea floor were carried out with the objective of determining the shear-wave velocities in the uppermost layers of marine sediments. In order to avoid underwater measurements, the shore belt was chosen as the experimental site. Explosives were detonated under low water cover on a shoal, geophones were mounted on land.

The experimental configuration and results are presented in the following two sections. It was not possible, using refraction seismic methods, to construct a clear model of the shear-wave velocities within the sea floor. It turns out that this difficulty results from the thinness of the uppermost sedimentary layer. On the other hand, the seismograms show the features of trapped surface modes. For this reason a dispersion analysis by means of multiple filter techniques was performed, and is described later. Following this, computations are presented which attempt to model the shear-wave velocity as a function of depth.

Experimental Configuration

The measurements were carried out in 1977 on the North Sea coast of the Federal Republic of Germany. Figure 1 shows the location of the area which was investigated.

Bore holes near the measured profile revealed that the holocene layer thickness is in the range 15–20 m (Barkhausen, Bundesanstalt für Geowissenschaften und Rohstoffe, Hannover, personal communication 1979). The essential constituents of the holocene are various sands and clays.

Figure 1 also shows the exact location of the record section and the positions of shot points and geophones. The shots were detonated on a shoal over a horizontal range of 1200 m with 100 m distance between adjacent points. In order to obtain maximum energy coupling the explosive charges were placed in flat holes during ebb-tide and detonated at flood-tide under a water cover of about 1 m. The size of the charges varied between 3 and 15 kg TNT. Six geophones were set up on the section line on land. The closest distance between a shot point and geophone was about 50 m. In the first part of the experiment the geo-

0340-062X/81/0049/0115/$01.60

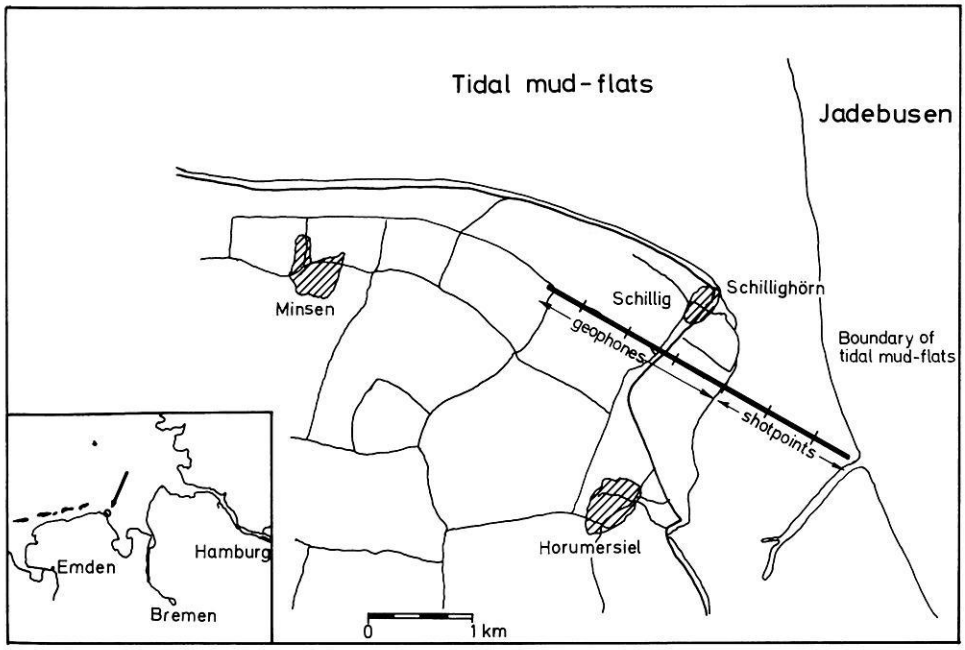

Fig. 1. Map of the experimental site

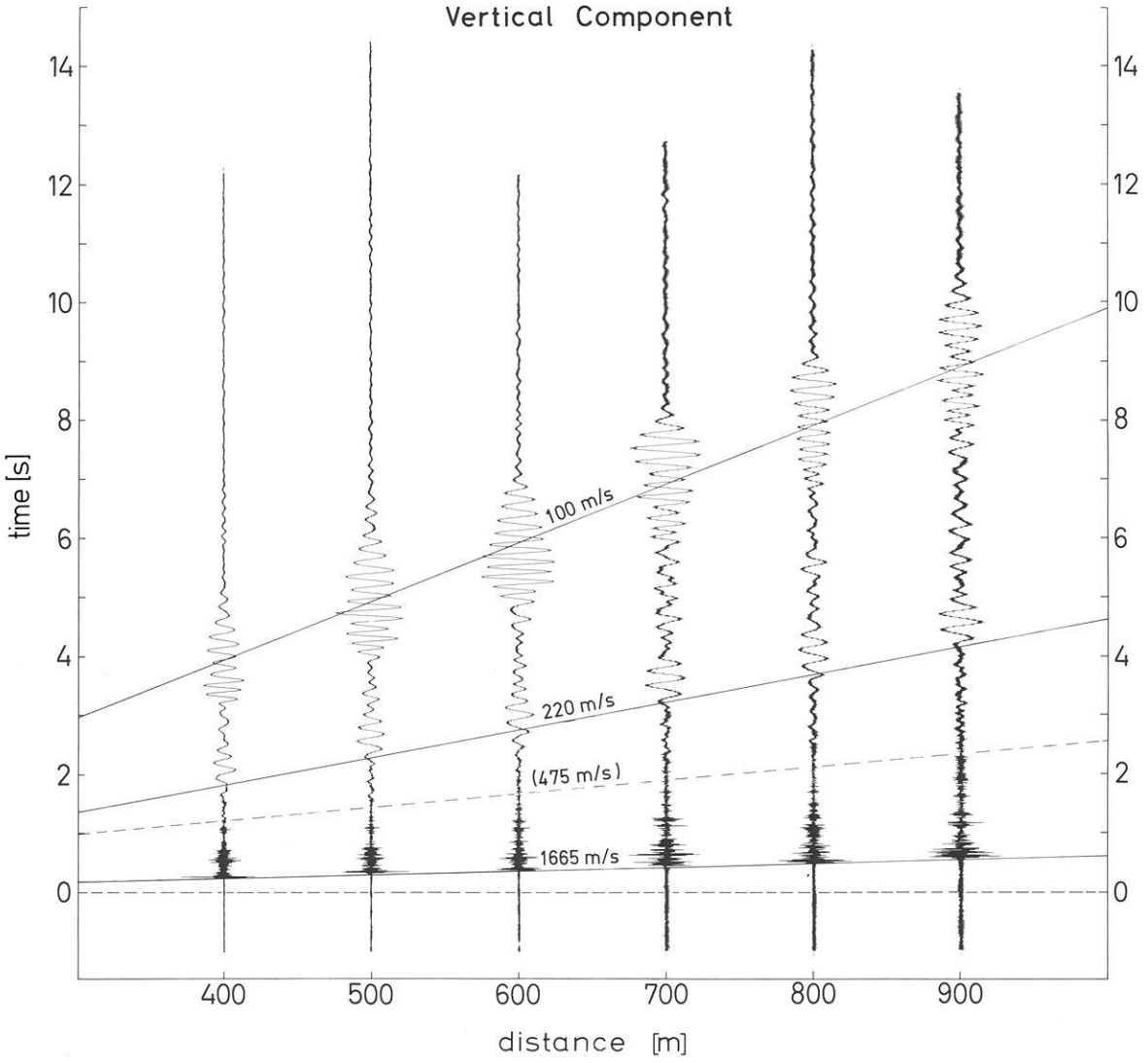

Fig. 2. Seismic section (shot points 12–17) for the fixed geophone G4, vertical component (*Z*)

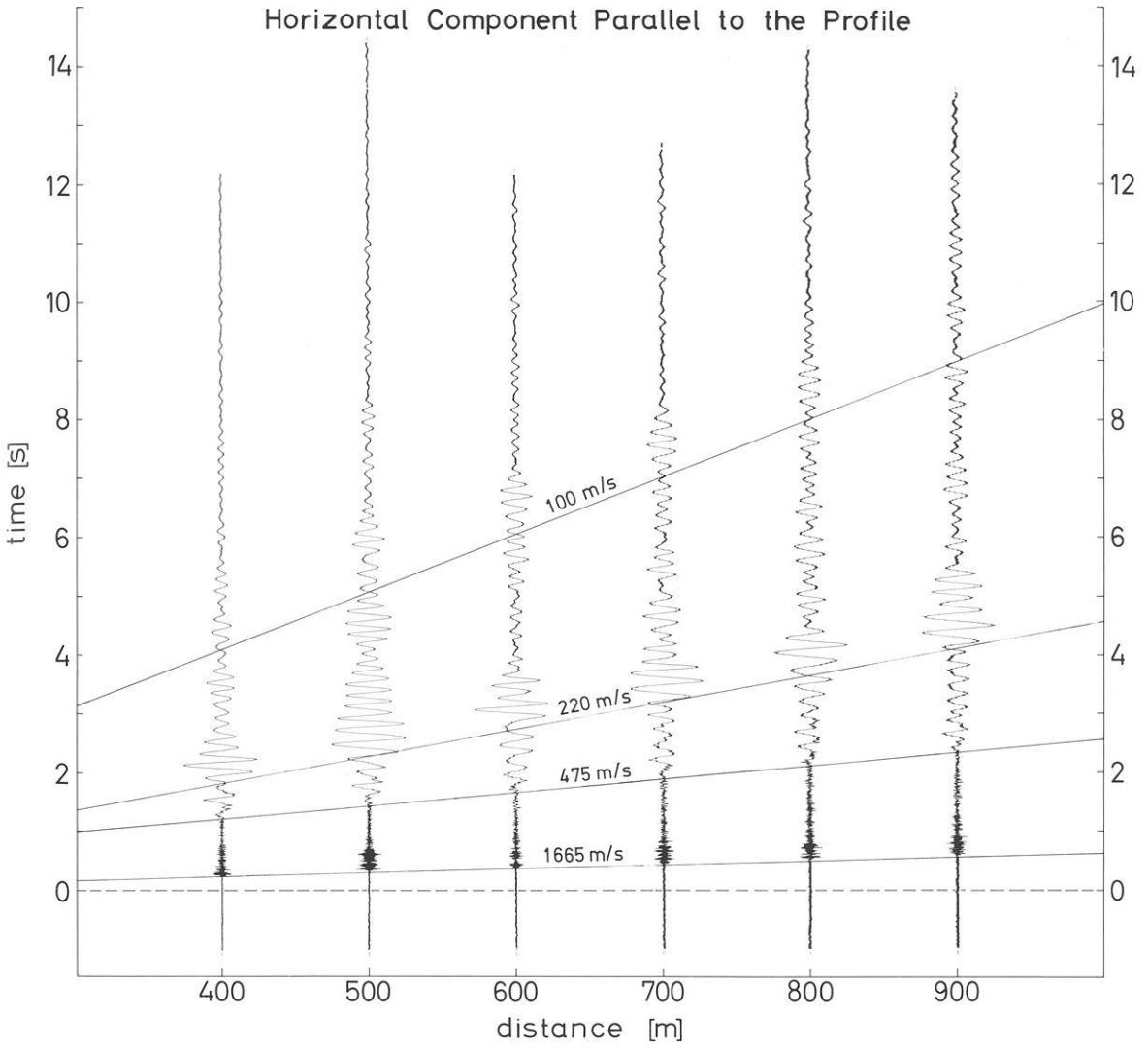

Fig. 3. Seismic section (shot points 12–17) for the fixed geophone G4, component in direction of profile (X)

phones were spread over 500 m on the profile line with a spacing of 100 m between adjacent geophones. In the second part the geophones were placed on a lengthened section line with a separation of 500 m, extending 1,500 m inland.

Geophones of the Geospace type with three components were used for the recordings. Their resonant frequency was 7.5 Hz. The data were recorded by FM equipment and telemetered by a UHF link to a central station.

Experimental Results

A total of 62 seismic sections were constructed. Thirty-two seismic sections were produced in such a way that the 6 geophones were combined with a fixed shotpoint for one section. For the remaining 30 sections seismograms from different shotpoints and a fixed geophone were combined. Comparisons of these types of representation showed that phase correlation between various shots for a fixed geophone delivered considerably better results. The coupling of the geophones with the soft and silty sand varied greatly. On the other hand, detonation occurred under relatively homogeneous conditions, since the charges were always set off near the surface under an approximately uniform water cover of about 1 m. The record sections were drawn separately for each component (Z: vertical, X: in the direction of profile, Y: perpendicular to profile). As an example we present the three sections in Figures 2–4 for shotpoints 12–17 and for the fixed geophone G4. The distance range extends from 0.4 km–0.9 km and the time range runs from 0 s (shot break) to 14 s.

A compressional wave velocity of $1{,}670 \pm 70\ \mathrm{ms}^{-1}$ was determined for most of the sections. As a result of several investigations we know that the compressional wave velocity for moist sand lies in the range of $1{,}600\ \mathrm{ms}^{-1}$ to $2{,}000\ \mathrm{ms}^{-1}$ (Schirmer et al. 1979).

The wave designated by $480\ \mathrm{ms}^{-1}$ is a refracted wave from a lower boundary layer. The portion comprising surface waves is well separated from these refraction events even for small offsets.

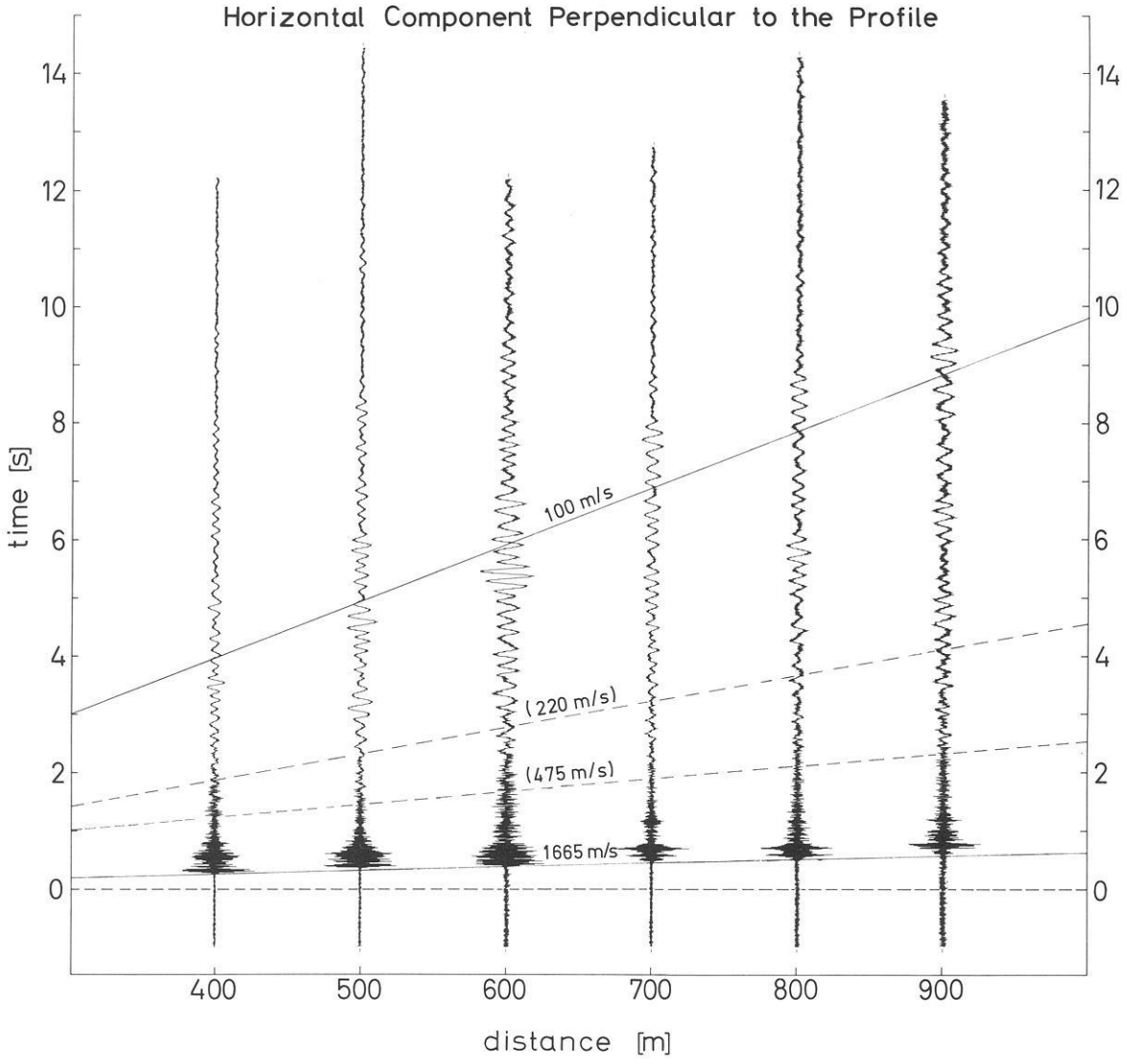

Fig. 4. Seismic section (shot points) 12–17) for the fixed geophone G4, component perpendicular to profile (Y)

Two velocities result from the many sections:

I: $100 \pm 10\ \mathrm{ms}^{-1}$

II: $230 \pm 20\ \mathrm{ms}^{-1}$.

Both are characteristic of the surface waves which were sought, i.e. the velocities of these surface waves are very low. Particle motions (hodographs) derived from the seismograms were computed. The following examples are shown:

I: for waves associated with a velocity of $100\ \mathrm{ms}^{-1}$ (Fig. 6)

II: for waves associated with a velocity of $230\ \mathrm{ms}^{-1}$ (Fig. 7),

each presented in the $X-Z$, $Y-Z$ and $X-Y$ planes. Figure 5 shows the respective seismograms. The particle motion is polarized in the $X-Z$ plane. The smoothness of the curve is attributed to the fact that the high-frequency portion of the spectrum is suppressed in the particle motion diagrams. By means of the hodographs, it was determined that both waves are of the Rayleigh type. The axial ratio amounted to:

I: $X/Z = 0.5 \pm 0.1$ (spread 0.33–0.65)
for waves associated with the velocity of $100\ \mathrm{ms}^{-1}$

II: $X/Z = 2.3 \pm 0.3$ (spread 1.7–2.6)
for waves associated with the velocity of $230\ \mathrm{ms}^{-1}$.

The first case (I) of surface waves involves an ellipse which is circumscribed clockwise, the second case (II) an ellipse which is circumscribed counter-clockwise.

Dispersion Analysis

The multiple filter technique is an efficient method of analyzing multi-mode dispersed signals. In this paper we follow the method of Dziewonski et al. (1969). The individual seismograms are filtered by a narrow bandpass at different center frequencies. This procedure is carried out by multiplying the Fourier-transformed time series with a Gaussian function. From the windowed spectrum the filtered in-phase and in-quadrature seismograms are obtained by inverse Fourier transformation. These

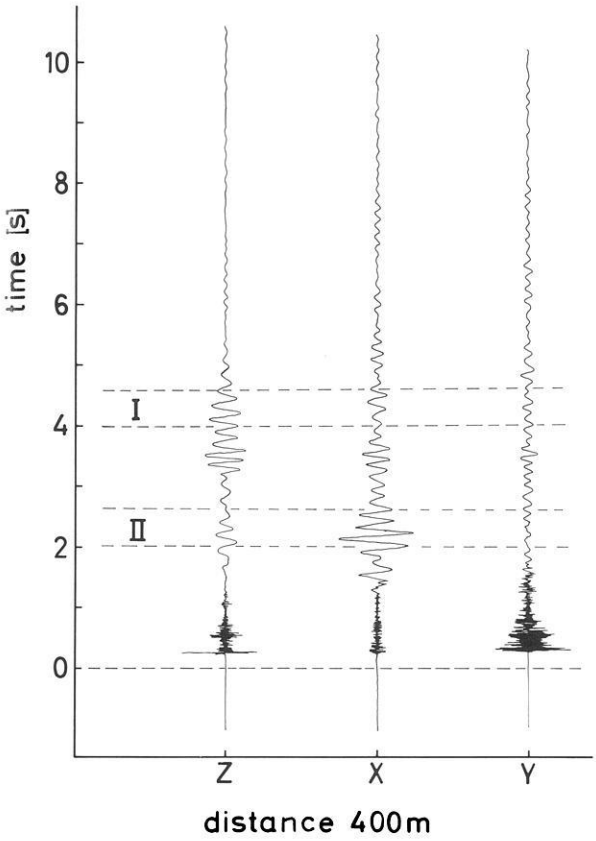

Fig. 5. Time series of seismograms in three components (Z vertical, X in direction of profile, Y perpendicular to profile) for a distance of 400 m between shot point and geophone. Particle motions were computed for sections I and II (Figs. 6 and 7)

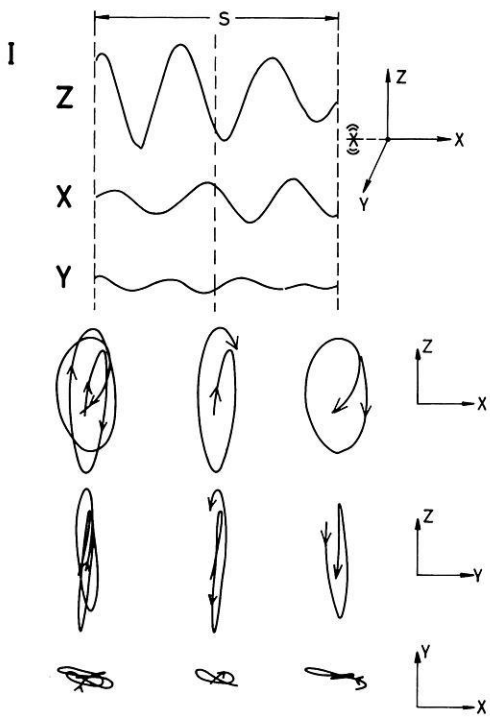

Fig. 6. Particle motion for the associated velocity of 100 ms^{-1} (Z vertical, X in direction of profile, Y perpendicular to profile, S section of seismogram in time domain, section I of Fig. 5)

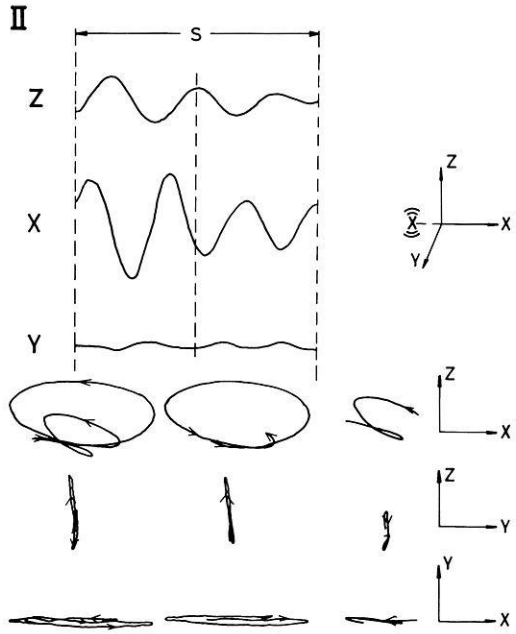

Fig. 7. Particle motion for the associated velocity of 230 ms^{-1} (Z vertical, X in direction of profile, Y perpendicular to profile, S section of seismogram in time domain, section II of Fig. 5)

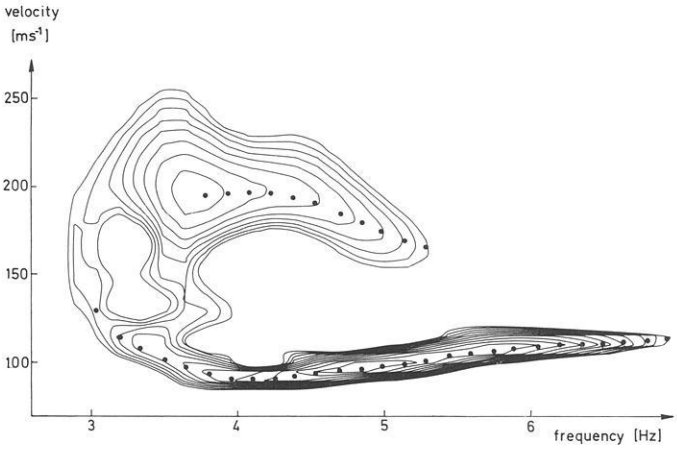

Fig. 8. Contours of the instaneous amplitude from the vertical component of particle velocity at 900 m distance, Fig. 2. The contours are drawn at 1 dB intervals, and the dots refer to the maxima of the amplitudes at the chosen center frequencies. Window function, (Dziewonski et al., 1969):

$$H(\omega,\omega_i)=\begin{cases}\exp\left(-100\left(\dfrac{\omega-\omega_i}{\omega_i}\right)^2\right) & \text{for } 0.8\cdot\omega_i\leqq\omega\leqq1.2\cdot\omega_i\\ 0 & \text{else}\end{cases}$$

time series yield the instantaneous amplitudes and phases as a function of time or propagation velocity. It may be shown that the maxima of the instantaneous amplitudes propagate approximately with the group velocity.

Figure 8 shows the contoured instantaneous amplitude as a function of frequency and group velocity from the vertical velocity component of geophone G4 at 900 m distance (Fig. 2).

Table 1. Axial ratios (ε) and phase differences ($\Delta\Phi$) of horizontal and vertical components of particle velocity, as derived from the filtered seismograms of Figs. 8 and 9

Center frequency {Hz}	1st mode		2nd mode	
	ε	$\Delta\Phi$	ε	$\Delta\Phi$
3.80	–	–	1.0	98°
3.95	–	–	1.3	105°
4.10	–	–	1.8	110°
4.25	–	–	2.1	113°
4.40	–	–	2.2	114°
4.55	0.35	−86°	2.3	113°
4.70	0.35	−89°	2.1	107°
4.85	0.35	−93°	2.1	100°
5.00	0.40	−95°	2.1	102°
5.15	–	–	2.1	110°

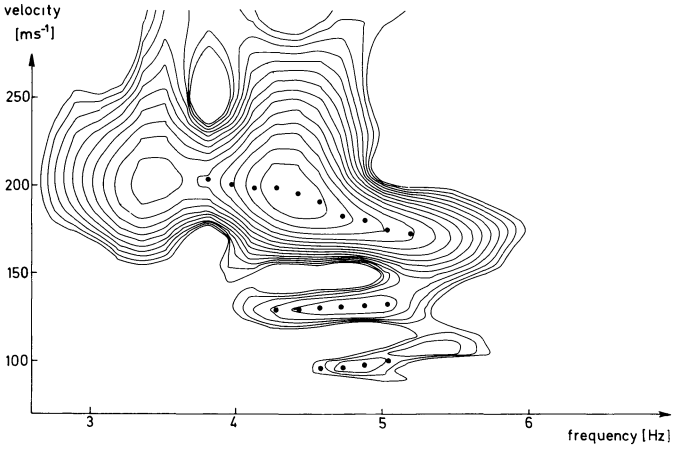

Fig. 9. Contours of the instantaneous amplitude from the in-line horizontal component of particle velocity at 900 m distance, Fig. 3. The contours are drawn at 1 dB intervals, and the dots refer to the maxima of the amplitudes at the chosen center frequencies. Window function: same as Fig. 8

The contours are drawn at 1 dB intervals, and the dots refer to the maxima of the filtered wave-group envelopes at the chosen center frequencies. As a result, it may be stated that there are at least two different modes of Rayleigh type. The analysis of further vertical velocity components at different distances and from other geophones yields similar contours. The resolution is not always as good, but the observed group velocities are the same, to within about 10%. This spread is the same as was obtained from the seismic sections (see previous section) and may be caused by the inhomogeneity of the sea floor.

The analysis of the velocity component parallel to the profile yields good agreement with respect to the (higher-velocity) 2nd mode, but the 1st mode can be observed only in the narrow frequency range 4.5–5.0 Hz (Fig. 9).

In Table 1 the axial ratios of horizontal and vertical amplitudes as well as the phase differences of the two components are presented for those frequencies where wave groups in both components are observed. A phase difference $\Delta\Phi$ of $-90°$ corresponds to clockwise and of 90° to counter-clockwise rotation (see next section). Thus, the results are in good agreement with the hodographs of the previous Chapter.

Figure 9 shows a third wave group which is found in the velocity component perpendicular to the profile. These waves may correspond to Love modes. Again, inhomogeneity of the sea floor might be responsible for Love-wave components parallel to the profile. A unique resolution of Love modes is not possible with our data. The main reason is the low energy of the velocity component perpendicular to the profile, which also seems to be influenced by the Rayleigh modes.

Model Calculations

The aim of this chapter is to find a model of shear-wave velocities in the sedimentary sea floor which allows the propagation of waves with the observed properties. These can be summarized as follows: the low-velocity part of the observed seismograms shows two different wave groups which propagate with velocities of about 100 and 230 ms $^{-1}$ and which are both of Rayleigh type, and the group velocities as well as the axial ratios of the particle motion have been obtained by dispersion analysis for a number of frequencies within the range 3.2–6.8 Hz. Furthermore it is known from borings that the thickness of the holocene layer is between 15 and 20 m at the experimental site. Thus, a discontinuous change of sedimentary parameters may be expected at this depth which is small compared with the horizontal propagation ranges of 100 to 2,500 m. For this reason the observed wave groups may be interpreted as trapped modes within the uppermost sedimentary layer. This assumption is in accordance with the observed dispersion, i.e., the frequency dependence of group velocity.

Considering a fixed position of the geophone at the water-sediment interface the Rayleigh-type modes may be described by,

$$u = \int_0^{\infty} \sum_{n=1}^{N(\omega)} G_n(\omega)\,\varepsilon_n(\omega)\cos\left\{\omega t - \phi_n(\omega) + \frac{\pi}{2}\right\} d\omega$$
$$w = \int_0^{\infty} \sum_{n=1}^{N(\omega)} G_n(\omega)\cos\{\omega t - \phi_n(\omega)\}\, d\omega \qquad (1)$$

with,

(u, w) = particle velocity, in-line horizontal component and vertical component, respectively
$G_n(\omega)$ = mode amplitudes
$\phi_n(\omega)$ = mode phases
$\varepsilon_n(\omega)$ = axial ratios of horizontal to vertical mode amplitudes

In our description we assumed the z-axis pointing upwards, so that a negative ε_n corresponds to an ellipse which is circumscribed clockwise. For comparison with Table 1, a difference of $-\pi/2$ or $\pi/2$ between horizontal and vertical phase means clockwise or counter-clockwise rotation, respectively.

The experimental results presented show waves, as described by Eq. (1), propagating along the water-sediment interface. From theoretical investigations it is known that such waves exist only for a non-zero shear-wave velocity in the sedimentary sea floor. As consequence of the measurements it can be assumed that the shear-wave velocity is smaller than the sound velocity in water, i.e.,

$$0 < \beta_s < \alpha_w < \alpha_s \qquad (2)$$

with,

α_w = sound velocity in water
β_s = shear-wave velocity in the sedimentary sea floor
α_s = compressional-wave velocity in the sedimentary sea floor

Considering a sea-floor model of a certain number of homogeneous layers of constant depth the group velocity may be determined theoretically as function of frequency. The simplest model which allows the propagation of interface waves consists of a water layer of constant depth overlying a homogeneous sedimentary halfspace. In this case the dispersion relation in accordance with Eq. (2) becomes,

$$\rho_w c^4 \gamma_s \tanh\left(\frac{\omega}{c}\gamma_w h\right) = \rho_s \beta_s^4 \gamma_w (4\gamma_s \hat{\gamma}_s - (1-\hat{\gamma}_s^2)^2) \qquad (3)$$

with,

$$\gamma_{w,s} = \left(1 - \left(\frac{c}{\alpha_{w,s}}\right)^2\right)^{\frac{1}{2}}, \quad \hat{\gamma}_s = \left(1 - \left(\frac{c}{\beta_s}\right)^2\right)^{\frac{1}{2}}$$

and,

h = water depth
$\rho_{w,s}$ = density of water and sediment, respectively
$\frac{\omega}{2\pi}$ = frequency
c = phase velocity

In the two limiting cases,

$\tanh\left(\frac{\omega}{c}\gamma_w h\right) = 0$ (no water coverage, Rayleigh waves)

$\tanh\left(\frac{\omega}{c}\gamma_w h\right) = 1$ (high water coverage, Scholte waves),

there is no dispersion, i.e., the phase velocity does not depend on frequency. Between these cases, where wavelength and water depth are of the same order of magnitude, the phase velocity depends on frequency. But computations show that this dispersion is weak. It turns out that even for more complicated sea-floor models, the influence of the water layer is of less importance. In the case of phase velocities which are small compared to that of sound in water ($c \ll \alpha_w$) the phase velocity is nearly independent of α_w and α_s. This result also holds for more complicated models.

In disagreement with our experimental results, the simple 1-layer sea-floor model allows the propagation of one mode only. This problem can be overcome by assuming the shear-wave velocity to increase with depth. Considering a number of discrete layers the well-known Thomson-Haskell matrix formalism can be applied in order to compute the dispersion relation, as in Schwab and Knopoff (1972). It should be noted that the conditions of Eq. (1) are different from usual seismic conditions where shear-wave velocities (of rocks) exceed the sound velocity of water.

First computations were carried out with a 2-layer sea-floor model covered by an additional water layer. As already mentioned the depth of the water layer as well as the compressional velocities of water and sediment have little influence on the group velocities. The same applies to the densities, within the reasonable limits known from experience. Thus, there are only three free parameters in our model: depth of the first sedimentary layer (the second one is a halfspace), and the shear-wave velocities in the two layers.

A lower limit to the layer depth is determined by the cutoff frequency of the second mode which should not be higher than 3.8 Hz (Fig. 8). In order to find a good fit to the observed group-velocities as a function of frequency, the so-called Hedgehog method is applied. The three free parameters are varied within the following ranges:

layer depth (1st layer): 15 m–20 m
shear-wave velocity (1st layer): 80 ms^{-1}–150 ms^{-1}
shear-wave velocity (2nd layer): 240 ms^{-1}–280 ms^{-1}

The theoretical group velocities are compared with the observed ones by means of a least-squares fit, where the observed values are represented by the dots in Fig. 8,

$$\sum_{\omega_i} \left(\frac{v_T - v_E}{v_T}\right)^2 = \min \qquad (4)$$

with,

v_T = theoretical group velocities } at the frequencies ω_i
v_E = observed group velocities } as defined by Fig. 8.

In this sum the group velocities of both modes are included. Due to the consideration of relative errors, higher absolute deviations are allowed for the (faster) second mode as compared to the first mode. This is in accordance with our observations which yield approximately the same percentage spread for the two mode velocities.

It turns out that there is only one well-defined minimum within the parameter ranges considered. The resolution of our method is 0.5 m with respect to the layer depth and 5 ms^{-1} with respect to the shear-wave velocities. Figure 10 shows the result of this group-velocity fit and also the corresponding axial ratios of horizontal and vertical amplitude. The corresponding model parameters are given in Table 2. Positive ω are related to counter-clockwise rotation and negative ω to clockwise rotation

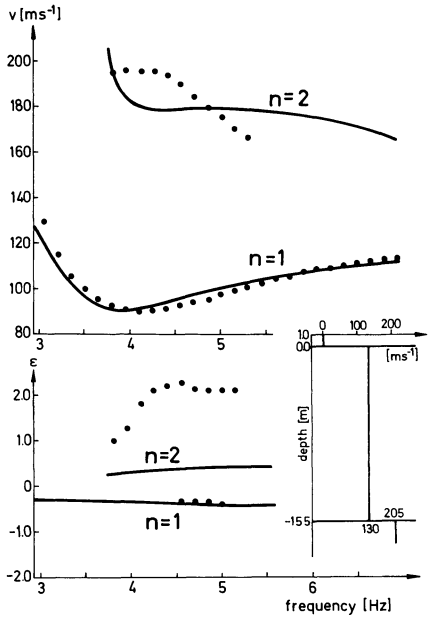

Fig. 10. Theoretical determination of group velocities (v) and axial ratios of horizontal and vertical amplitude (ε) for a two-layer sea-floor model. The dots refer to the observed values as presented in Fig. 8 and Table 1, respectively. Model parameters are given in Table 2

Table 2. Parameters of best-fit 2-layer model

Model parameters	h[m]	ρ[gcm^{-3}]	α[ms^{-1}]	β[ms^{-1}]
Covering water layer	1	1	1,500	0
1st sedimentary layer	15.5	1.8	1,700	130
2nd sedimentary layer	∞	1.9	1,800	205

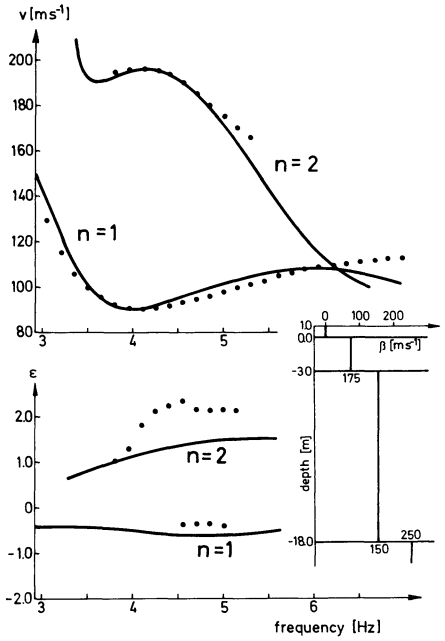

Fig. 11. Theoretical determination of group velocities (v) and axial ratios of horizontal and vertical amplitude (ε) for a 3-layer sea-floor model. The dots refer to the observed values as presented in Fig. 8 and Table 1, respectively. Model parameters are given in Table 3

Table 3. Parameters of best-fit 3-layer model

Model parameters	h[m]	ρ[gcm ^{3}]	α[ms^{-1}]	β[ms^{-1}]
Covering water layer	1	1	1,500	0
1st sedimentary layer	3	1.8	1,700	75
2nd sedimentary layer	15	1.8	1,700	150
3rd sedimentary layer	∞	1.9	1,800	250

(see Eq. (1)). The agreement of computed and observed group velocities is good for the first mode but not satisfactory for the second mode. The same applies to the particle motion where the direction of rotation as well as the axial ratios for the first mode are well-predicted by theory, but the axial ratios differ considerably for the second mode. Numerical tests show that this discrepancy cannot be overcome within the 2-layer sea-floor model. Thus it is necessary to modify the model.

One possibility is to introduce a gradient in the shear-wave velocity in the first layer, which requires only one more model parameter. But a number of numerical experiments did not yield satisfactory results. For this reason a 3-layer model is investigated, which requires two additional model parameters as compared to the 2-layer model.

Equation (4) is used for the 3-layer model also, in order to obtain an optimal fit to group velocities. It turns out that the discrepancy in second-mode axial ratios may be reduced by considering a near-surface layer of lower shear-wave velocity. In this model the agreement of first-mode group velocities may be maintained and improved for second-mode group velocities. Figure 11 and Table 3 show the best fitting model. Still the agreement of computed and observed axial ratios is not optimal, especially with respect to the second mode. But this deviation might be explained by the several shortcomings of the experiment, and it is not meaningful to investigate more sophisticated models. First of all the sea floor is not homogeneous, and while the group velocity is a mean value with respect to the whole propagation range the particle motion is influenced mainly by the local constitution of the sea floor. Furthermore variation in the quality of coupling for the different geophone components in the sediment may produce errors in the measured axial ratios.

Conclusions

Comparison of the experimental results with model calculations shows satisfactory agreement. By means of a relatively simple model, consisting of three homogeneous layers within the sea floor, we are able to interpret the propagation velocities and axial ratios of particle motion including the direction of circumscription of the ellipses. This is a surprising result because the upper layers of the sea floor are usually not at all homogeneous. Borings and sea floor probes in the North Sea show quite large variations of physical parameters such as compressional wave velocity and density. Also our seismic measurements yield different velocities at different ranges within the same area. For this reason the model presented describes only a vertically and horizontally averaged shear-wave velocity profile.

The values from 75 ms^{-1} to 250 ms^{-1} in the region of the uppermost 20 m yield ratios of compressional- to shear-wave velocity in the range from 21 to 6.5, which agree well with the measurements of Hamilton et al. (1970). Our model also compares well with the depth dependence of shear-wave velocities as reviewed by Hamilton (1976). Our result is of interest with respect to underwater acoustics as shear-wave velocities of 250 ms^{-1} may contribute considerably to low-frequency sound attenuation in shallow water (Essen, 1977).

Acknowledgements. The authors are indebted to the Erprobungsstelle E71 der Bundeswehr for their help during the measurements. We also thank Professor Behle for helpful discussions and Dr. Barkhausen who made the bore-hole data available to us. The work was supported by the Sonderforschungsbereich 94, the Bundesminister für Verteidigung and the Bundesminister für Forschung und Technologie.

References

Cagniard, L.: Reflection and refraction of progressive seismic waves, pp. 244–246. New York: McGraw-Hill 1962

Dziewonski, A., Bloch, S., Landisman, M.. A technique for the analysis of transient seismic signals, Bull. Seismol. Soc. Am. **59**, 427–444, 1969

Essen, H.-H.: Attenuation coefficients of acoustic normal modes in shallow water. J. Geophys. **43**, 569–580, 1977

Hamilton, E.L.: Shear-wave velocity versus depth in marine sediments: a review. Geophysics **41**, 985–996, 1976

Hamilton, E.L.: Bucker, H.P., Keir, D.L., Whitney, J.A.: Velocities of compressional and shear waves in marine sediments determined in situ from a research submersible. J. Geophys. Res. **75**, 4039–4049, 1970

Hawker, K.E.: The existence of Stoneley waves as a loss mechanism in plane wave reflection problems. J. Acoust. Soc. Am. **65**, 682–686, 1979

Schirmer, F., Schmalfeldt, B., Siebert, J.: Schallgeschwindigkeit und Impedanz des oberen Meeresbodens in Gebieten der Nordsee, des Skagerraks, des Kattegatts und der Ostsee. Dt. hydrogr. Z. **32**, 279–288, 1979

Schwab, F.A., Knopoff, L.: Fast surface wave and free mode computations, In: Methods of computational physics, **11**, 87–180. New York, London: Academic Press 1972

Received June 11, 1979; Revised Version August 19, 1980
Accepted September 10, 1980